

Electronic Supplementary Information for “Pattern formation, localized and running pulsation on active spherical membranes”

Subhadip Ghosh[†], Sashideep Gutti^{*}, and Debasish Chaudhuri^{‡, •}

[†]Department of Physics, Faculty of Science, University of Zagreb, Bijenika cesta 32,
10000 Zagreb, Croatia

^{*}BITS Pilani Hyderabad Campus, Hyderabad 500078, Telengana, India

[‡]Institute of Physics, Sachivalaya Marg, Bhubaneswar 751005, India

[•]Homi Bhabha National Institute, Anushaktinagar, Mumbai 400094, India

September 10, 2021

1 Additional Phase Diagrams and time evolutions

All the simulations are performed at a fixed bending modulus $\tilde{\kappa} = 25$, attachment rate $\tilde{k}_{on} = 3 \times 10^4$, detachment rate $\tilde{k}_0 = 10$, and spread parameter of myosin pull $\alpha = 0.001$. In Fig.1 in this ESI, we explore the impact of changing active parameter \tilde{f}_r and the passive stabilizing factor of surface tension $\tilde{\sigma}$ keeping \tilde{f}_p fixed. Due to the positive $\tilde{H} = 1$, clustering of APs pull in the membrane locally. The active reaction \tilde{f}_r due to F-actin polymerization, on the other hand, pushes the membrane outward. The surface tension $\tilde{\sigma}$ acts as a stabilizing factor.

Fig. 2 of ESI shows localized pulsation corresponding to the excitation of $l = 3$ mode at $\tilde{f}_r = 94.5$, $\tilde{\sigma} = 113$ corresponding to region (iii) of Fig.3(a) in the main text. The corresponding kymograph in Fig. 3 of ESI shows the evolution of u and ψ along the polar angle θ at a fixed $\phi = \pi/2$.

In the main text, we have shown a kymograph of running pulsation at $\phi = \pi/2$ in Fig. 7. In Fig. 4 of ESI, we complement it with the kymograph at $\phi = \pi$ corresponding to the same set of parameter values, displaying the connected running pulsations. Along with Fig. 7 of the main text, Fig. 4 shows that the local flux corresponding to the traveling wave depends on the location (θ, ϕ) .

Fig. 5 of ESI shows parametric plots comprising of deformation field u and local AP density field ψ corresponding to running pulsation at a fixed set of θ and ϕ locations on top of the sphere. The parameter values are listed in figure caption, and correspond to Fig.7 in the main text. We note the existence of multiple periodicity at different locations, and the difference in amplitude of the oscillations in r and ψ at various (θ, ϕ) points.

The l -mode dependence of real and imaginary parts of eigenvalues $\lambda_{2,3}$ distinguish the nature of stable, linearly unstable, and unstable spiral phases. This is shown in Fig. 6 of ESI, corresponding to the running pulsation at parameter values corresponding to Figs 7 and 11 of the main text.

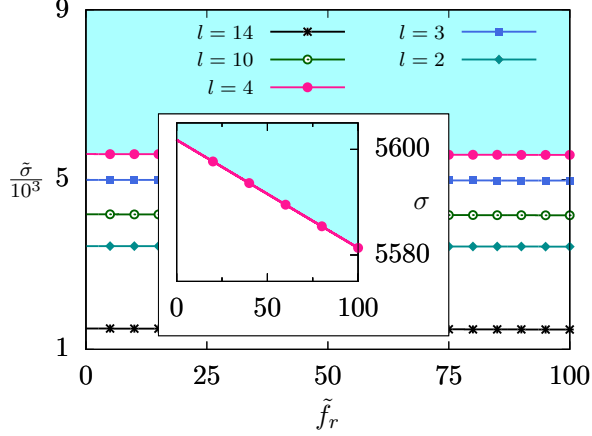


Figure 1: Phase diagram for spherical membrane, using valley preferring APs with $\tilde{H} > 0$ in $\tilde{\sigma} - \tilde{f}_p$ plane showing dynamical transition from linearly stable (s) to unstable (u) phase indicating pattern formation. As the actomyosin pull gets coupled with inward curvature producing APs, it brings about linear instability in the system through a positive feedback. Parameter values are, $\tilde{H} = 1$, and a fixed $\tilde{f}_p = 10$, $\tilde{\mu} = 0.02$, $\tilde{K}_t = 2000$. All other parameters are fixed as in Table-1 of the main text. Each line corresponds to a s - u boundary for a specific l -mode as indicated in the figure legend. In the region above these lines the system is stable corresponding to the particular l -mode. The shaded region is linearly stable for all l modes.

Finally in Fig. 7 of ESI we depict conformational changes due to linear instability corresponding to the phase diagram Fig.8 of the main text, at $\tilde{\sigma} = 530$, $\tilde{f}_p = 5.0$, where $l = 2$ mode is unstable. The corresponding evolution is qualitatively similar to the deformations of a cell at cytokinesis.

2 Choice of parameters

The cell can change its size and shape by regulating the osmotic pressure and effective surface tension. The bare surface tension σ of such membranes can be $\sim 1 \text{ pN}/\mu\text{m}$ [1]. This is tunable, e.g., the surface tension can be reduced incorporating more cholesterol in the membrane.

The actin polymerization rate at barbed end is $\sim 7.4 \mu\text{M}^{-1}\text{s}^{-1}$. With changing actin concentration from zero to $4 \mu\text{M}$ it varies between $\approx 2 - 30$ subunit/s [4]. Considering subunit size $\sim 2.76 \text{ nm}$ the actin growth rate gives a velocity $v_g = 5.52$ to 82.8 nm/s . To directly translate it to protrusion of spherical membrane of radius $r_0 = 10 \mu\text{m}$, the relative growth rate $f_r = v_g/r_0$ is $\sim 5 \times 10^{-4} - 8 \times 10^{-3} \text{ s}^{-1}$. A myosin drive of F-actin with velocity $v_p \sim 1 \mu\text{m/s}$ [5], leads to $f_p = v_p/r_0 \sim 0.1 \text{ s}^{-1}$.

The viscosity of cytoplasmic extract is $\eta \sim 10 \text{ mPa}\cdot\text{s}$ [6]. the viscous friction coefficient turns out to be $\gamma \approx 3\pi\eta\xi \approx 2.8 \times 10^{-9} \text{ N s/m} = 2.8 \times 10^{-3} \text{ pN}\cdot\text{s}/\mu\text{m}$ assuming the thickness of actin cortex $\xi \approx 30 \text{ nm}$ [7]. Using the radius of spherical membrane $r_0 = 10 \mu\text{m}$ we get the membrane mobility coefficient $\Gamma = 1/\gamma r_0^2 \approx 3.57 (\text{pN } \mu\text{m s})^{-1}$.

The two dimensional diffusivity of AP is $\sim 1 \mu\text{m}^2/\text{s}$ [8, 9]. Considering a vesicle of radius $r_0 \approx 10 \mu\text{m}$ this gives the angular diffusivity $D = 1 \mu\text{m}^2\text{s}^{-1}/r_0^2 = 10^{-2} \text{ s}^{-1}$. Table-1 gives

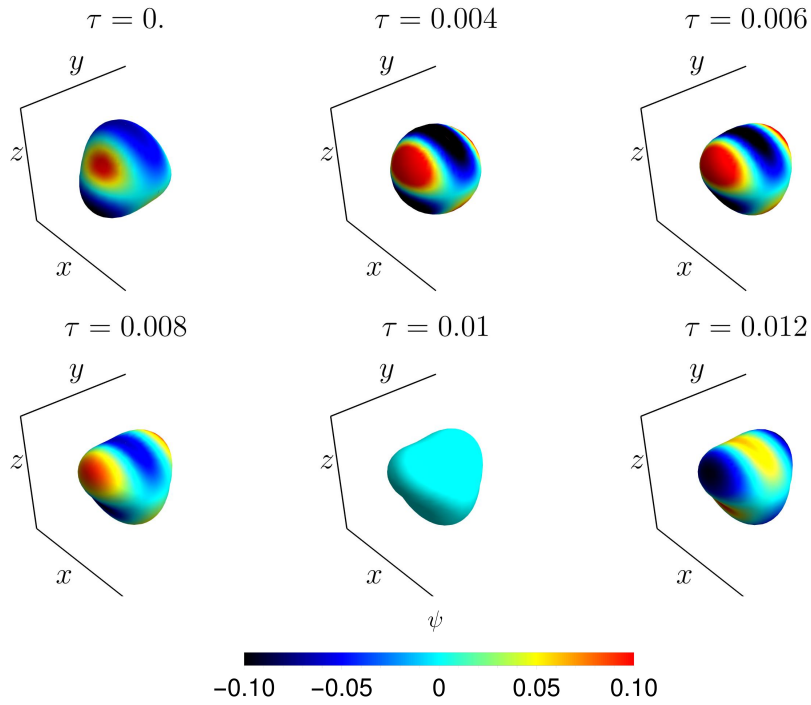


Figure 2: Plots showing localized pulsations corresponding to $l = 3$ mode for a spherical membrane in which the APs prefer hills. The color code on the deforming spherical shapes denotes the local AP concentration ψ . The parameter values used are $\tilde{H} = -1$, $\tilde{\mu} = 0.15$, $\tilde{K}_t = 1000$, $\tilde{\sigma} = 113$, $\tilde{f}_r = 94.5$, $\tilde{f}_p = 50$.

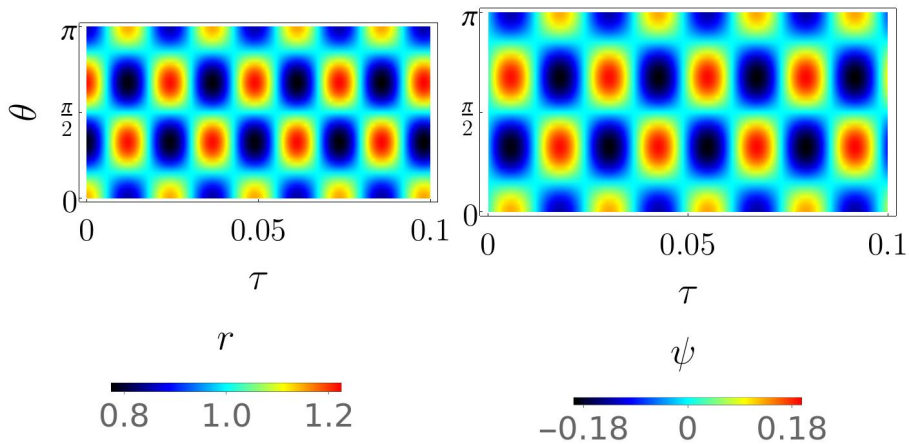


Figure 3: Kymographs depicting the time evolution over azimuthal angle θ at $\phi = \frac{\pi}{2}$. The parameter values used are $\tilde{H} = -1$, $\tilde{\mu} = 0.15$, $\tilde{K}_t = 1000$, $\tilde{\sigma} = 113$, $\tilde{f}_r = 94.5$, $\tilde{f}_p = 50$.

the list of parameter values used in the numerical calculations in this paper.

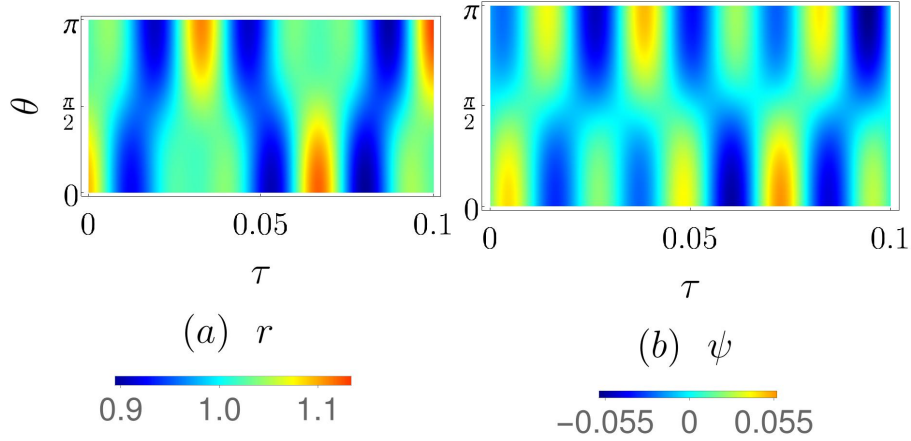


Figure 4: Kymographs of running pulsation corresponds to Fig. 7 of main text. It shows evolutions of membrane deformation $r = r_0(1 + u)$ and change in AP concentration ψ over the polar angle θ at a fixed $\phi = \pi$. A running pulsation is generated with superposition of $l = 2, 3$ modes. The parameter values used here are $\tilde{H} = -1$, $\tilde{\mu} = 0.15$, $\tilde{K}_t = 10^3$, $\tilde{f}_p = 50$, $\tilde{\sigma} = 60$ and $\tilde{f}_r = 75$ corresponding to Fig. 7 and 11 of the main text. The connected nature of deformations is due to the traveling wave, and their slopes with respect to time indicate the velocities.

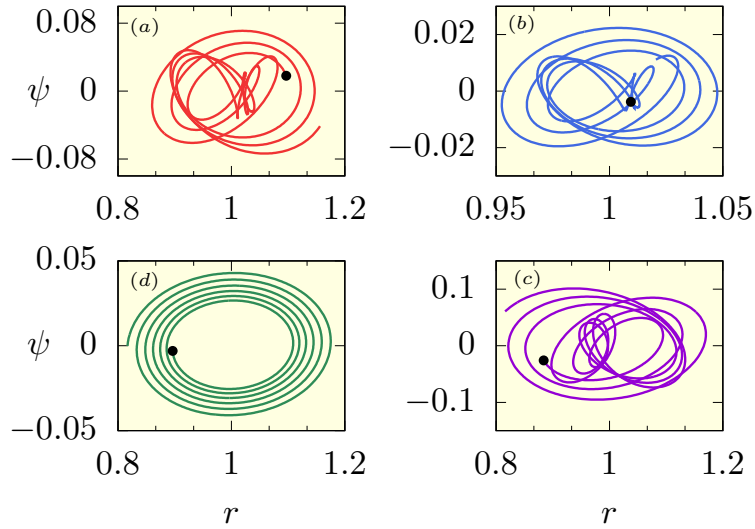


Figure 5: Parametric plots of the field variables $r = r_0(1 + u)$ and ψ showing oscillations with multiple periodicity as the system displays traveling waves on the membrane surface. The plots display the behavior at azimuthal angles (a) $\theta = 0$, (b) $\theta = \frac{\pi}{6}$, (c) $\theta = \frac{\pi}{3}$ and (d) $\theta = \frac{\pi}{2}$. The parameter values used are $\tilde{H} = -1$, $\tilde{\mu} = 0.15$, $\tilde{K}_t = 10^3$, $\tilde{f}_p = 50$, $\tilde{\sigma} = 60$ and $\tilde{f}_r = 75$, as in Fig. 7 of the main text. The filled black \circ in each plot indicates the initial state.

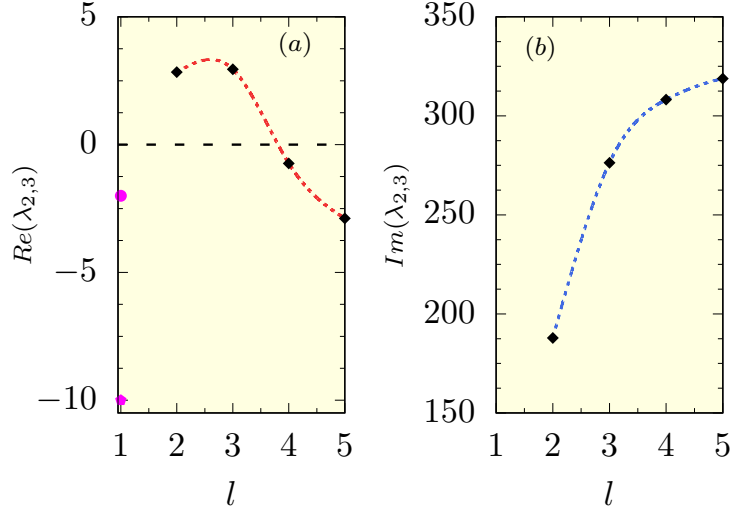


Figure 6: The eigenvalues corresponding to running pulsation in Fig. 7 of main text. The parameter values used are $\tilde{H} = -1$, $\tilde{\mu} = 0.15$, $\tilde{K}_t = 10^3$, $\tilde{f}_p = 50$, $\tilde{\sigma} = 60$ and $\tilde{f}_r = 75$. $\lambda_{2,3}$ are purely real and negative for $l = 1$ and are denoted by the filled symbols \diamond (λ_2) and \circ (λ_3). They have complex conjugate values with real part shown in (a) and the imaginary part in (b) using the filled \diamond symbol. $\lambda_1 < 0$ for all l .

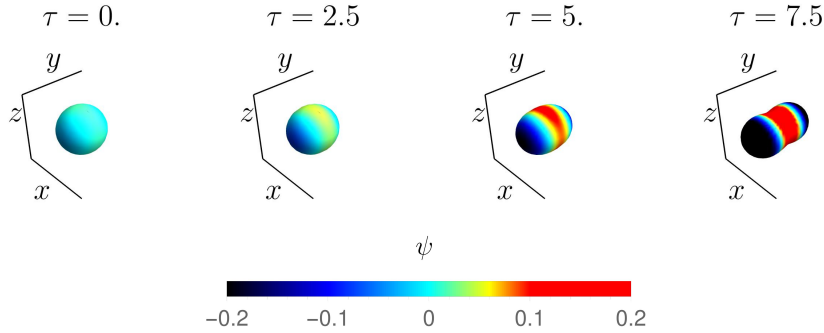


Figure 7: Plots showing pattern formation on a spherical membrane due to linear instability in $l = 2$ mode with $\tilde{H} = 1$, i.e., when the APs prefer local valleys. The color code on the deforming spherical shapes denotes the local AP concentration ψ . The parameter values used are $\tilde{\mu} = 0.02$, $\tilde{K}_t = 2000$, $\tilde{f}_r = 10$, as in Fig.8 of main text, with $\tilde{\sigma} = 530$, $\tilde{f}_p = 5.0$.

3 Description of videos

The three video in the ESI depict the time evolution in the three distinct dynamical regimes of the spherical membrane predicted by our model. The consecutive frames in localized pulsation (local_pulse.avi), and the running pulsation (run_pulse.avi) are separated by dimensionless time gaps $\Delta\tau = 10^{-4}$ and $\Delta\tau = 2 \times 10^{-4}$, respectively. In the main text, snapshots from these movies are depicted in Figs 5, 6 and Figs 7, 11 respectively. The figure captions

Parameters	Definition	Values	Scaled parameters	Scaled values
D [s^{-1}]	angular diffusivity	10^{-2}	unit	
r_0 [μm]	radius	10	unit	
Γ [($\text{pN } \mu\text{m s}$) $^{-1}$]	membrane mobility	1.0	unit	
\bar{H} [μm^{-1}]	AP induced curvature	± 0.1 [8]	$\tilde{H} = \bar{H}r_0$	± 1
μ [($\text{pN } \mu\text{m s}$) $^{-1}$]	AP mobility	0.5, 0.07	$\tilde{\mu} = \frac{\mu}{\Gamma}$	0.15, 0.02
σ [$\text{pN}/\mu\text{m}$]	bare surface tension	$0 - 2$ [1]	$\tilde{\sigma} = \frac{\sigma r_0^2 \Gamma}{D}$	$0 - 2 \times 10^4$
κ [$k_B T$]	bending modulus	60 [10]	$\tilde{\kappa} = \frac{\kappa \Gamma}{D}$	25
K_t [$\text{pN}/\mu\text{m}^3$]	tether	0.001, 0.002 [11]	$\tilde{K}_t = \frac{K_t r_0^4 \Gamma}{D}$	1000, 2000
f_r [s^{-1}]	actin polymerization	$0 - 1$ [4]	$\tilde{f}_r = \frac{f_r}{D}$	$0 - 100$
f_p [s^{-1}]	myosin contraction	$0 - 1$ ($\mathcal{O}[f_r]$)	$\tilde{f}_p = \frac{f_p}{D}$	$0 - 100$
k_{on} [s^{-1}]	attachment rate	300 [8]	$\tilde{k}_{\text{on}} = \frac{k_{\text{on}}}{D}$	3×10^4
k_0 [s^{-1}]	bare detachment rate	0.1 [8]	$\tilde{k}_0 = \frac{k_0}{D}$	10

Table 1: The table lists all the parameters and their typical values used in the numerical calculations. r_0 , D , and Γ set the units of length, time and force in the calculations.

mention the values of the parameters used.

On the other hand, the consecutive frames in the movie of pattern formation due to linear instability (pattern.avi) is separated by $\Delta\tau = 5 \times 10^{-3}$. The snapshots from this movie and corresponding parameter values are shown in Fig.9 of the main text.

References

- [1] T. Betz and C. Sykes, *Soft Matter* **8**, 5317 (2012).
- [2] A. G. Clark, O. Wartlick, G. Salbreux, and E. K. Paluch, *Curr. Biol.* **24**, R484 (2014).
- [3] G. Salbreux, G. Charras, and E. Paluch, *Trends Cell Biol.* **22**, 536 (2012).
- [4] J. R. Kuhn and T. D. Pollard, *Biophys. J.* **88**, 1387 (2005).
- [5] S. J. Kron and J. A. Spudich, *Proc. Natl. Acad. Sci. U. S. A.* **83**, 6272 (1986).
- [6] M. Valentine, Z. Perlman, T. Mitchison, and D. Weitz, *Biophys. J.* **88**, 680 (2005).
- [7] A. G. Clark, K. Dierkes, and E. K. Paluch, *Biophys. J.* **105**, 570 (2013).
- [8] R. Shlomovitz and N. S. Gov, *Phys. Rev. Lett.* **98**, 168103 (2007).
- [9] C. H. Chen, F. C. Tsai, C. C. Wang, and C. H. Lee, *Phys. Rev. Lett.* **103**, 238101 (2009).
- [10] J. Agudo-Canalejo and R. Golestanian, *New Journal of Physics* **19**, 125013 (2017).
- [11] R. Alert, J. Casademunt, J. Brugués, and P. Sens, *Biophys. J.* **108**, 1878 (2015).